

## Supporting Information

### Understanding the Dopant Induced Effects on SFX-MeOTAD for Perovskite Solar Cells: A Spectroscopic and Computational Investigation

Fraser Gunn<sup>a</sup>, Paheli Ghosh<sup>b</sup>, Michal Maciejczyk<sup>c</sup>, Joseph Cameron<sup>d</sup>, Dennis Nordlund<sup>e</sup>, Satheesh Krishnamurthy<sup>b</sup>, Tell Tuttle<sup>a</sup>, Peter J. Skabara<sup>d</sup>, Neil Robertson<sup>c</sup>, and Aruna Ivaturi<sup>a\*</sup>

<sup>a</sup>Smart Materials Research and Device Technology (SMaRDT) Group, WestCHEM, Department of Pure and Applied Chemistry, University of Strathclyde, Thomas Graham Building, Glasgow, G1 1XL, United Kingdom

<sup>b</sup>School of Engineering & Innovation, The Open University, Milton Keynes, MK7 6AA, United Kingdom

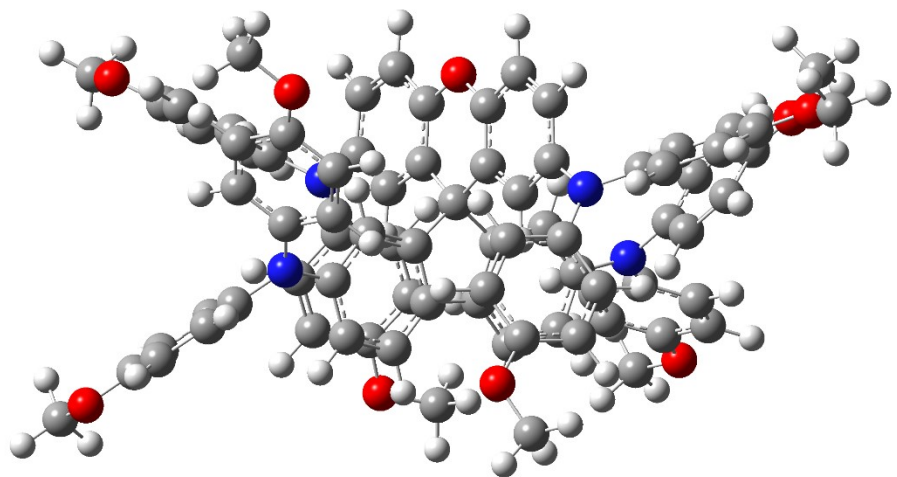
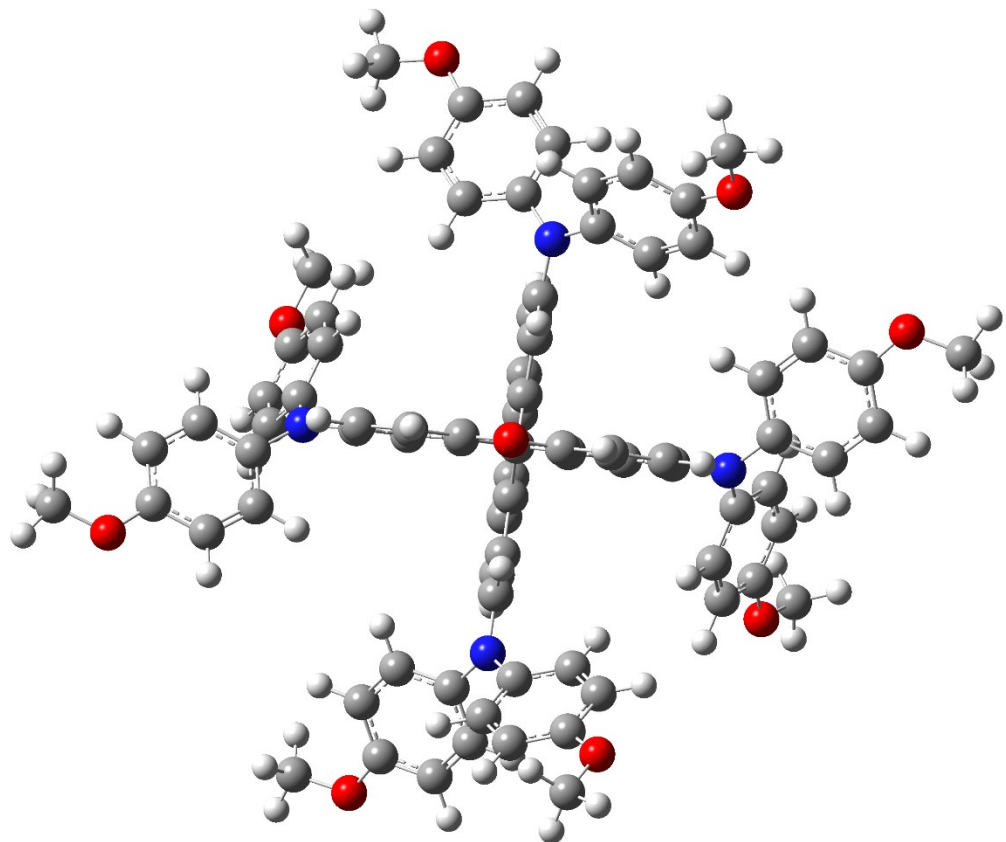
<sup>c</sup>School of Chemistry, University of Edinburgh, King's Buildings, Edinburgh, EH93FJ, United Kingdom

<sup>d</sup> WestCHEM, School of Chemistry, University of Glasgow, Joseph Black Building, University Place, Glasgow, G12 8QQ, United Kingdom

<sup>e</sup>Stanford Synchrotron Radiation Lightsource, SLAC National Accelerator Laboratory, Menlo Park, CA 94025, USA

\*aruna.ivaturi@strath.ac.uk

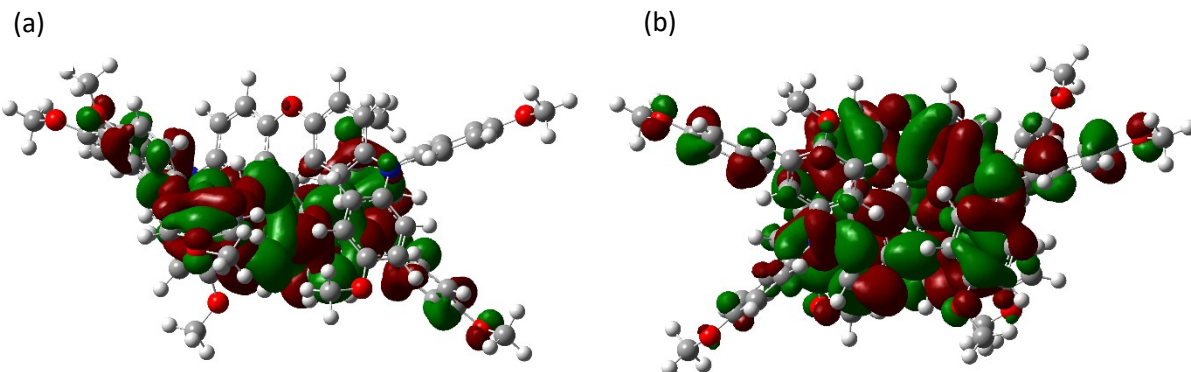
**S1:** Optimised molecular structure of SFX-MeOTAD in two different views



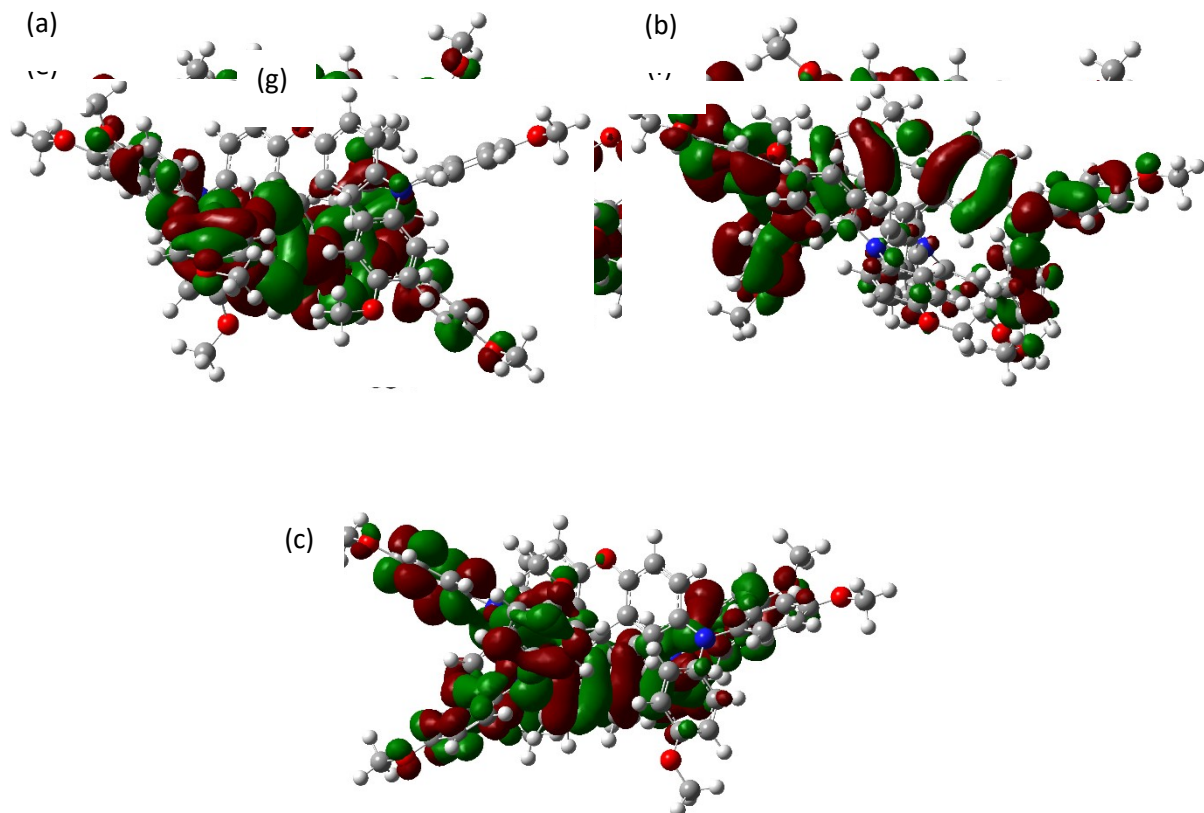
**S2:** Molecular orbital energies (eV) of SFX-MeOTAD, SFX-MeOTAD<sup>+</sup>, SFX-MeOTAD<sup>2+</sup> and SFX-MeOTAD<sup>4+</sup> in chlorobenzene

Energy Level	SFX-MeOTAD	SFX-MeOTAD <sup>+</sup>		SFX-MeOTAD <sup>2+</sup>		SFX-MeOTAD <sup>4+</sup>	
		$\alpha$	$\beta$	$\alpha$	$\beta$	$\alpha$	$\beta$
L+7 (335)	-0.205	-0.830	-0.776	-1.254	-1.182	-2.276	-2.141
L+6 (334)	-0.234	-0.857	-0.825	-1.357	-1.253	-2.319	-2.249
L+5 (333)	-0.422	-0.910	-0.834	-1.485	-1.420	-2.466	-2.410
L+4 (332)	-0.574	-1.010	-0.987	-1.590	-1.520	-2.574	-2.454
L+3 (331)	-0.720	-1.203	-1.200	-1.873	-1.771	-2.786	-2.772
L+2 (330)	-0.785	-1.336	-1.264	-1.951	-1.839	-2.891	-2.805
L+1 (329)	-0.816	-1.562	-1.455	-1.977	-1.876	-2.992	-2.925
L (328)	-1.025	-1.935	-1.770	-2.308	-2.153	-3.353	-3.339
H (327)	-4.870	-5.265	-4.535	-6.075	-4.889	-5.629	-5.522
H-1 (326)	-4.926	-5.492	-5.263	-6.111	-5.023	-7.290	-5.654
H-2 (325)	-5.166	-5.775	-5.491	-6.437	-5.731	-7.421	-5.686
H-3 (324)	-5.337	-6.292	-5.794	-6.591	-6.086	-7.460	-7.405
H-4 (323)	-6.419	-6.787	-6.786	-7.404	-7.270	-8.086	-8.077
H-5 (322)	-6.467	-6.889	6.885	-7.536	-7.308	-8.488	-8.121
H-6 (321)	-6.597	-6.916	-6.913	-7.546	-7.336	-8.509	-8.127
H-7 (320)	-6.613	-7.175	-6.966	-7.554	-7.462	-8.525	-8.327

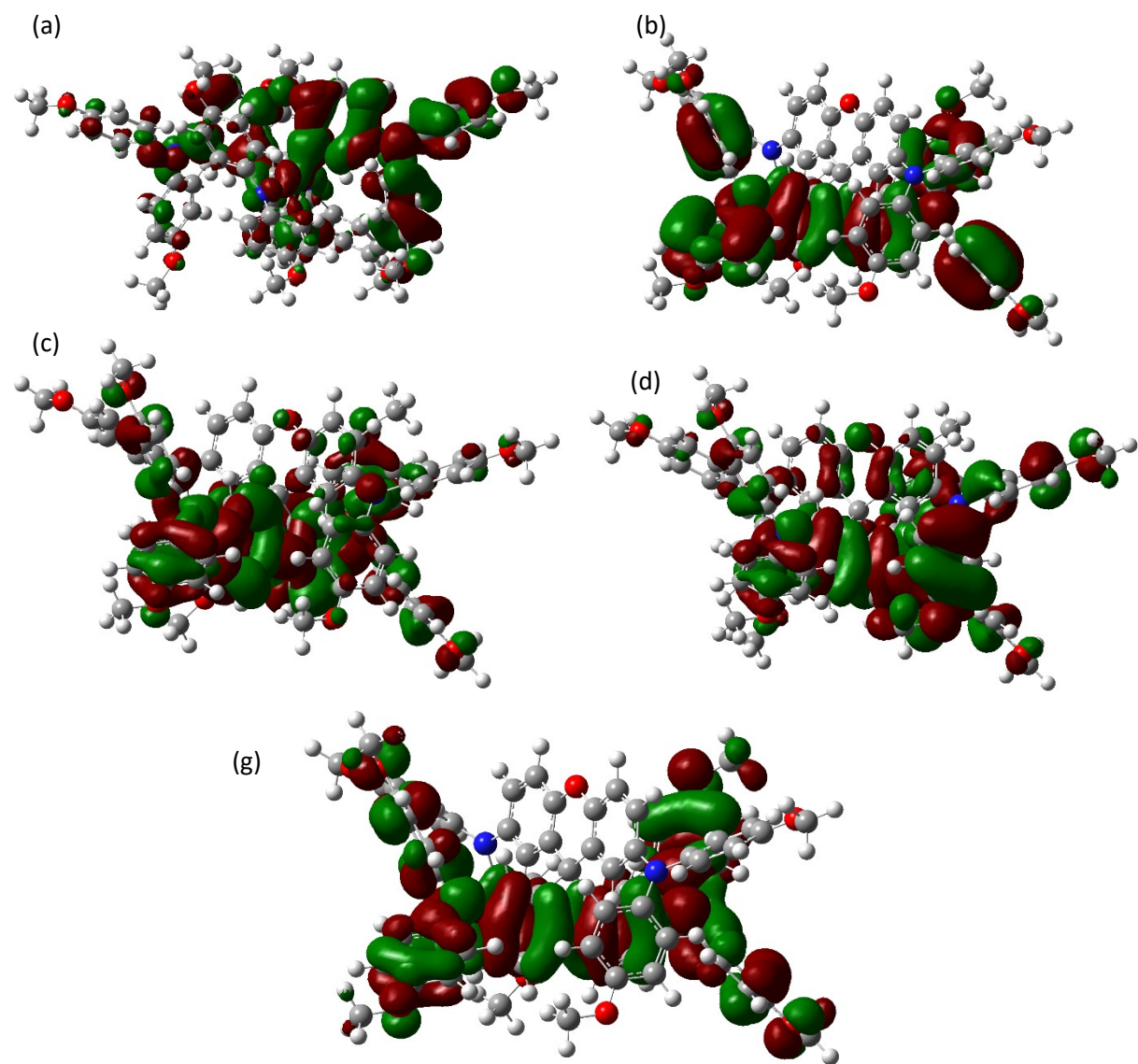
**S3:** Isodensity representations of HOMO-LUMO together for each SFX-MeOTAD species in chlorobenzene solvent: (a) HOMO-LUMO of neutral SFX-MeOTAD; (b)  $\alpha$ -HOMO-LUMO of SFX-MeOTAD<sup>+</sup>; (c)  $\beta$ -HOMO-LUMO of SFX-MeOTAD<sup>+</sup>; (d)  $\alpha$ -HOMO-LUMO of SFX-MeOTAD<sup>2+</sup>; (e)  $\beta$ -HOMO-LUMO of SFX-MeOTAD<sup>2+</sup>; (f)  $\alpha$ -HOMO-LUMO of SFX-MeOTAD<sup>4+</sup>; (g)  $\beta$ -HOMO-LUMO of SFX-MeOTAD<sup>4+</sup>



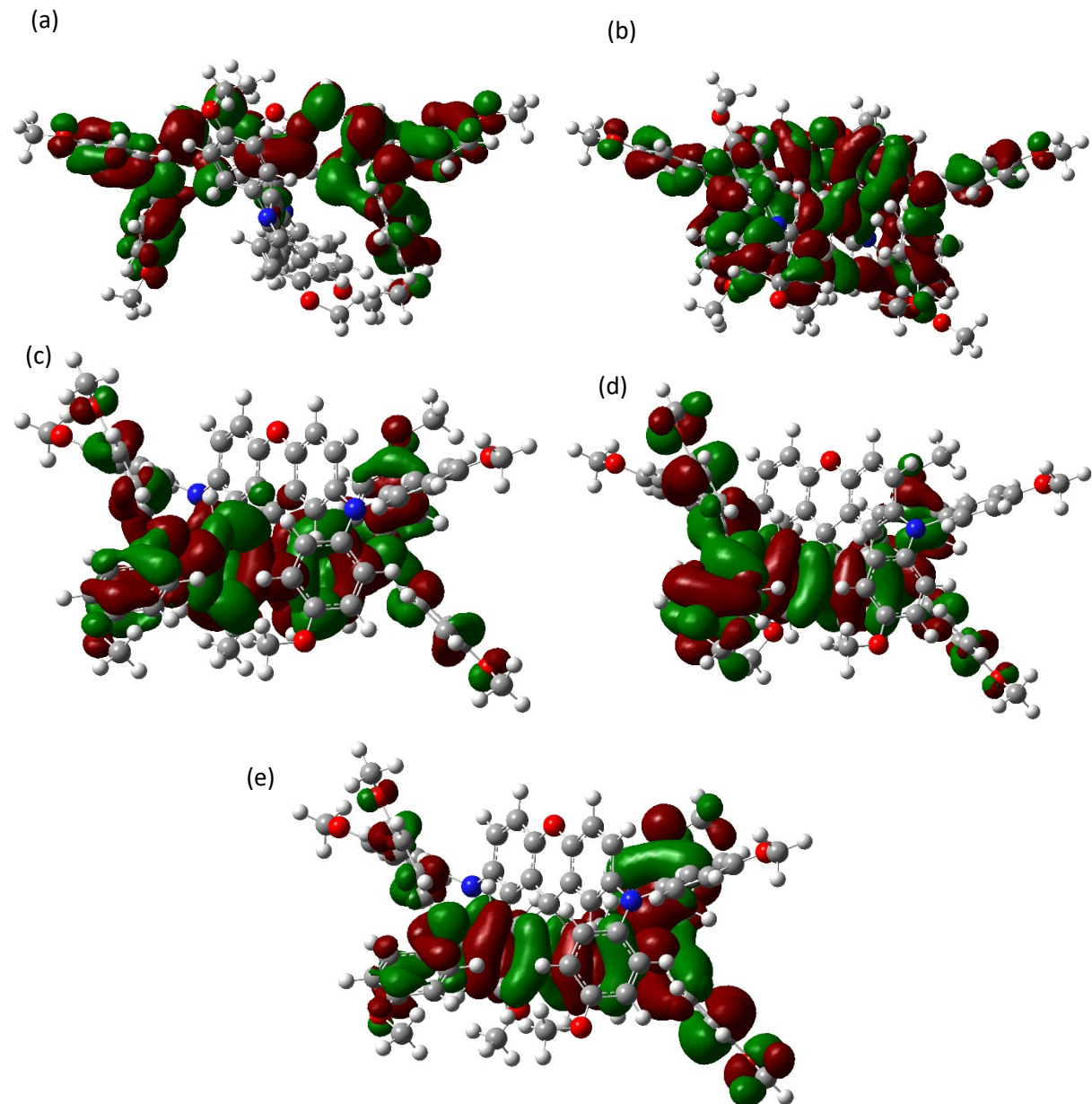
**S4:** Isodensity representations of transitions for neutral SFX-MeOTAD in chlorobenzene (transitions combined): (a) HOMO->LUMO; (b) HOMO-1 MO+11; (c) HOMO->LUMO+8



**S5:** Isodensity representations of transitions for SFX-MeOTAD<sup>2+</sup> in chlorobenzene (transitions are combined): (a) HOMO $\alpha$ ->LUMO+3 $\alpha$ ; (b) HOMO-13 $\beta$ ->LUMO+1 $\beta$ ; (c) HOMO-1 $\alpha$ ->LUMO $\alpha$ ; (d) HOMO-7 $\beta$ ->LUMO $\beta$ ; (e) HOMO-5 $\beta$ ->LUMO+1 $\beta$



**S6:** Isodensity representations of transitions for SFX-MeOTAD<sup>+</sup> in chlorobenzene (transitions are combined): (a) HOMO-1 $\alpha$ ->LUMO+3 $\alpha$ ; (b) HOMO $\alpha$ ->LUMO+2 $\alpha$ ; (c) HOMO-2 $\alpha$ ->LUMO $\alpha$ ; (d) HOMO-8 $\beta$ ->LUMO $\beta$ ; (e) HOMO-7 $\beta$ ->LUMO $\beta$





**S7:** Energy, wavelength, oscillator strength (f) and composition of the TDDFT excitation states of neutral SFX-MeOTAD in chlorobenzene. For each state, the percentage orbital contributions of the TDDFT eigenvalues are reported. The orbital contributions were obtained using the Gausssum 3.0.2 software.<sup>1</sup>

States	Energy (eV)	Wavelength (nm)	f	Major Contributions	Minor Contributions
1	3.1018	399.72	1.2397	HOMO->LUMO (96%)	
25	4.0328	307.44	0.435	H-2->L+4 (11%), H-1->L+11 (37%)	H-2->L+6 (3%), H-2->L+8 (7%), H-2->L+10 (2%), H-2->L+11 (9%), H-1->L+10 (9%), HOMO->L+10 (5%)
22	3.9965	310.23	0.3235	H-3->L+1 (14%), H-1->L+8 (13%), H-1->L+10 (15%), HOMO->L+8 (18%)	H-3->L+9 (3%), H-2->L+6 (3%), H-2->L+8 (6%), H-2->L+10 (8%), H-1->L+11 (2%), HOMO->L+10 (5%)
8	3.5540	348.86	0.2979	H-1->L+2 (63%)	H-1->L+5 (10%), H-2->LUMO (2%), H-2->L+1 (5%), H-1->L+3 (7%), H-1->L+4 (5%)
9	3.5855	345.8	0.2691	H-2->LUMO (35%), H-1->L+2 (24%), H-1->L+3 (16%)	H-2->L+1 (4%), H-1->L+4 (6%), H-1->L+5 (9%)
23	4.0009	309.89	0.2658	H-3->L+1 (28%), H-1->L+8 (15%), HOMO->L+10 (14%)	H-3->L+9 (4%), H-2->L+6 (2%), H-2->L+8 (3%), H-2->L+10 (4%), H-2->L+11 (2%), H-1->L+10 (4%), H-1->L+11 (4%), HOMO->L+8 (5%), HOMO->L+11 (2%)
27	4.1121	301.51	0.1758		H-1->L+15 (10%), HOMO->L+6 (10%) H-2->L+3 (3%), H-2->L+4 (5%), H-2->L+5 (6%), H-2->L+6 (4%), H-2->L+11 (4%), H-2->L+15 (4%), H-1->L+6 (8%), H-1->L+11 (7%), H-1->L+12 (7%), H-1->L+14 (3%), H-1->L+16 (3%), HOMO->L+12 (6%), HOMO->L+13 (2%)
10	3.6053	343.89	0.1752	H-2->LUMO (59%)	H-2->L+1 (9%), H-1->L+2 (5%), H-1->L+3 (6%), H-1->L+4 (7%), H-1->L+5 (8%)
18	3.9137	316.8	0.1411	H-1->L+3 (14%), H-1->L+5 (60%)	H-2->L+1 (4%), H-2->L+2 (2%), H-2->L+3 (2%), H-1->L+4 (8%)
33	4.1615	297.93	0.1274	H-2->L+6 (16%), H-1->L+16 (29%)	H-2->L+4 (7%), H-2->L+14 (6%), H-2->L+15 (4%), H-1->L+6 (7%), H-1->L+14 (6%), HOMO->L+6 (3%)
21	3.9883	310.87	0.1166	H-3->L+2 (15%), HOMO->L+9 (47%)	H-3->L+1 (6%), H-3->L+8 (4%), H-3->L+9 (5%), HOMO->L+5 (4%), HOMO->L+8 (6%)
24	4.0135	308.91	0.1156	H-3->L+1 (41%), HOMO->L+9 (14%), HOMO->L+10 (12%)	H-3->L+2 (3%), H-3->L+8 (3%), H-3->L+10 (3%), H-1->L+11 (3%), HOMO->L+8 (8%)
32	4.1439	299.2	0.1016	H-1->L+14 (14%), HOMO->L+6 (18%)	H-2->L+14 (10%), H-1->L+12 (10%), H-2->L+4 (3%), H-2->L+5 (5%), H-2->L+15 (2%), H-1->L+6 (9%), HOMO->L+13 (8%)
34	4.1885	296.01	0.0835	H-2->L+4 (22%), H-2->L+5 (25%), H-1->L+7 (13%)	H-2->L+3 (2%), H-2->L+12 (2%), H-2->L+16 (3%), H-1->L+6 (3%), H-1->L+12 (3%), H-1->L+14 (2%), H-1->L+15 (6%), H-1->L+16 (8%), H-1->L+17 (3%)
6	3.4598	358.36	0.0621	H-3->L+2 (14%), HOMO->L+3 (59%), HOMO->L+4 (15%)	HOMO->L+1 (2%), HOMO->L+5 (2%)

**S8:** Energy, wavelength, oscillator strength (f) and composition of the TDDFT excitation states of SFX-MeOTAD<sup>+</sup> in chlorobenzene. For each state, the percentage orbital contributions of the TDDFT eigenvalues are reported. The orbital contributions were obtained using the Gausssum 3.0.2 software.<sup>1</sup>

States	Energy (eV)	Wavelength (nm)	f	Major Contributions	Minor Contributions
3	0.6819	1818.11	0.8475	H-2(B)->LUMO(B) (99%)	
17	2.7309	454	0.519	H-2(A)->LUMO(A) (63%)	H-7(A)->LUMO(A) (2%), HOMO(A)->LUMO(A) (9%), H-19(B)->LUMO(B) (5%), H-15(B)->LUMO(B) (6%)
48	3.4757	356.72	0.1997	H-1(A)->L+3(A) (16%)	HOMO(B)->L+3(B) (10%), HOMO(B)->L+7(B) (10%) H-1(A)->L+11(A) (5%), HOMO(A)->L+2(A) (4%), HOMO(A)->L+14(A) (2%), HOMO(A)->L+18(A) (4%), H-1(B)->L+2(B) (8%), H-1(B)->L+4(B) (7%), H-1(B)->L+12(B) (6%), HOMO(B)->L+5(B) (4%), HOMO(B)->L+16(B) (3%)
47	3.4590	358.44	0.1175	HOMO(A)->L+2(A) (14%), H-1(B)->L+4(B) (13%)	H-1(A)->L+3(A) (8%), H-1(A)->L+11(A) (7%), HOMO(A)->L+4(A) (8%), HOMO(A)->L+6(A) (5%), HOMO(A)->L+7(A) (4%), HOMO(A)->L+14(A) (2%), HOMO(A)->L+18(A) (2%), H-1(B)->L+2(B) (3%), H-1(B)->L+12(B) (6%), HOMO(B)->L+7(B) (2%), HOMO(B)->L+16(B) (4%), HOMO(B)->L+18(B) (2%)
42	3.3441	370.76	0.1109	HOMO(A)->L+2(A) (34%), HOMO(B)->L+3(B) (20%), HOMO(B)->L+5(B) (12%)	H-1(A)->L+3(A) (5%), HOMO(A)->L+3(A) (4%), HOMO(A)->L+4(A) (7%), H-1(B)->L+4(B) (6%), HOMO(B)->L+4(B) (5%)
8	2.0101	616.82	0.1056	H-7(B)->LUMO(B) (95%)	H-8(B)->LUMO(B) (3%)
9	2.0486	605.22	0.1021	H-8(B)->LUMO(B) (95%)	H-7(B)->LUMO(B) (3%)
18	2.7498	450.88	0.051	HOMO(A)->LUMO(A) (89%)	H-2(A)->LUMO(A) (6%)
14	2.5798	480.59	0.0346	H-18(B)->LUMO(B) (30%), H-15(B)->LUMO(B) (48%)	H-2(A)->LUMO(A) (4%), H-22(B)->LUMO(B) (2%), H-21(B)->LUMO(B) (3%), H-19(B)->LUMO(B) (5%), H-17(B)->LUMO(B) (4%)
41	3.3253	372.85	0.0296	H-2(A)->L+2(A) (16%), H-2(B)->L+2(B) (18%)	H-3(A)->L+1(A) (7%), H-3(A)->L+8(A) (6%), H-2(A)->L+6(A) (3%), H-2(A)->L+7(A) (4%), H-2(A)->L+8(A) (2%), H-23(B)->LUMO(B) (3%), H-2(B)->L+9(B) (6%)
40	3.3032	375.34	0.0281	HOMO(A)->L+3(A) (38%), HOMO(B)->L+4(B) (37%)	H-1(A)->L+4(A) (3%), HOMO(A)->L+2(A) (4%), H-1(B)->L+5(B) (3%), HOMO(B)->L+3(B) (5%)
46	3.4355	360.89	0.0258	H-2(A)->L+2(A) (12%), H-2(B)->L+2(B) (18%)	H-3(A)->L+1(A) (4%), H-3(A)->L+5(A) (4%), H-3(A)->L+8(A) (4%), H-2(A)->L+6(A) (5%), H-2(A)->L+7(A) (5%), H-6(B)->L+8(B) (2%), H-2(B)->L+1(B) (2%), H-2(B)->L+6(B) (4%), H-2(B)->L+9(B) (6%)
53	3.5617	348.1	0.0255	HOMO(A)->L+2(A) (11%), HOMO(B)->L+3(B) (21%)	H-1(A)->L+19(A) (3%), HOMO(A)->L+4(A) (5%), HOMO(A)->L+7(A) (2%), HOMO(A)->L+16(A) (3%), HOMO(A)->L+17(A) (4%), H-1(B)->L+2(B) (2%), H-1(B)->L+4(B) (3%), H-1(B)->L+16(B) (2%), HOMO(B)->L+5(B) (2%), HOMO(B)->L+16(B) (2%), HOMO(B)->L+17(B) (2%)
13	2.5174	492.5	0.0242	H-18(B)->LUMO(B) (39%), H-15(B)->LUMO(B) (38%)	H-2(A)->LUMO(A) (2%), H-22(B)->LUMO(B) (4%), H-21(B)->LUMO(B) (5%), H-19(B)->LUMO(B) (3%), H-17(B)->LUMO(B) (2%), H-16(B)->LUMO(B) (3%), H-11(B)->LUMO(B) (2%)
56	3.6179	342.7	0.0239		H-6(A)->L+13(A) (2%), H-3(A)->LUMO(A) (3%), H-2(A)->L+2(A) (2%), H-1(A)->L+2(A) (4%), H-1(A)->L+17(A) (2%), HOMO(A)->L+2(A) (6%), HOMO(A)->L+4(A)

				(4%), HOMO(A)->L+18(A) (2%), H-5(B)->L+14(B) (2%), H-2(B)->L+1(B) (2%), H-2(B)->L+2(B) (5%), H-1(B)->L+17(B) (2%), HOMO(B)->L+3(B) (6%), HOMO(B)->L+18(B) (2%), HOMO(B)->L+23(B) (2%)
--	--	--	--	---

**S9:** Energy, wavelength, oscillator strength (f) and composition of the TDDFT excitation states of SFX-MeOTAD<sup>2+</sup> in chlorobenzene. For each state, the percentage orbital contributions of the TDDFT eigenvalues are reported. The orbital contributions were obtained using the Gausssum 3.0.2 software.<sup>1</sup>

States	Energy (eV)	Wavelength (nm)	f	Major Contributions	Minor Contributions
4	0.6401	1937.09	0.8526	H-1(B)->L+1(B) (99%)	
28	2.7021	458.84	0.4601	H-1(A)->LUMO(A) (45%), H-13(B)->L+1(B) (22%)	H-16(B)->L+1(B) (10%), H-6(A)->LUMO(A) (2%), HOMO(A)->LUMO(A) (8%), H-10(B)->L+1(B) (2%)
1	0.2929	4232.81	0.4475	HOMO(B)->LUMO(B) (100%)	
49	3.1831	389.51	0.2189	HOMO(A)->L+3(A) (19%), HOMO(B)->L+3(B) (13%)	H-2(A)->L+1(A) (2%), H-2(A)->L+3(A) (9%), H-2(A)->L+5(A) (2%), H-1(A)->L+3(A) (2%), HOMO(A)->LUMO(A) (2%), HOMO(A)->L+1(A) (7%), HOMO(A)->L+4(A) (2%), HOMO(A)->L+5(A) (3%), HOMO(B)->L+5(B) (7%), HOMO(B)->L+18(B) (2%)
29	2.7134	456.93	0.1651	H-1(A)->LUMO(A) (17%), H-13(B)->L+1(B) (69%)	HOMO(A)->LUMO(A) (3%), H-10(B)->L+1(B) (2%)
8	1.7880	693.44	0.1536	H-7(B)->LUMO(B) (50%), H-4(B)->LUMO(B) (41%)	H-2(B)->LUMO(B) (8%)
11	1.9473	636.71	0.1258	H-6(B)->L+1(B) (34%), H-5(B)->L+1(B) (62%)	
9	1.7984	689.42	0.105	H-7(B)->LUMO(B) (42%), H-4(B)->LUMO(B) (42%), H-3(B)->LUMO(B) (12%)	H-2(B)->LUMO(B) (2%)
12	1.9854	624.48	0.1043	H-6(B)->L+1(B) (63%), H-5(B)->L+1(B) (35%)	
17	2.2373	554.17	0.0539	H-8(B)->LUMO(B) (94%)	H-11(B)->LUMO(B) (2%)
56	3.3329	372	0.0315	H-2(A)->L+6(A) (21%), HOMO(B)->L+8(B) (18%)	H-9(A)->L+21(A) (2%), H-2(A)->L+4(A) (2%), H-2(A)->L+8(A) (8%), HOMO(A)->L+6(A) (2%), HOMO(B)->L+4(B) (3%), HOMO(B)->L+6(B) (3%), HOMO(B)->L+10(B) (5%), HOMO(B)->L+11(B) (2%)
21	2.4833	499.27	0.0303	H-10(B)->L+1(B) (91%)	H-1(A)->LUMO(A) (3%)
7	1.7519	707.72	0.0271	H-3(B)->LUMO(B) (65%), H-2(B)->LUMO(B) (16%)	H-7(B)->LUMO(B) (7%), H-5(B)->LUMO(B) (2%), H-4(B)->LUMO(B) (2%), H-3(B)->L+1(B) (5%)
5	1.6097	770.23	0.0248	H-4(B)->LUMO(B) (13%), H-2(B)->LUMO(B) (71%)	H-3(B)->LUMO(B) (10%), H-3(B)->L+1(B) (4%)
60	3.3882	365.93	0.0203		H-8(A)->L+17(A) (2%), H-8(A)->L+20(A) (2%), H-3(A)->L+7(A) (5%), H-3(A)->L+9(A) (8%), H-3(A)->L+10(A) (3%), H-1(A)->L+7(A) (5%), H-1(A)->L+9(A) (9%), H-1(A)->L+10(A) (3%), H-1(B)->L+9(B) (5%), H-1(B)->L+10(B) (4%), H-1(B)->L+11(B) (4%), H-1(B)->L+12(B) (4%)
48	3.1775	390.19	0.0191	H-21(B)->LUMO(B) (46%)	HOMO(A)->L+3(A) (10%), H-2(A)->L+1(A) (3%), H-2(A)->L+4(A) (2%), H-1(A)->L+1(A) (2%), HOMO(A)->L+1(A) (7%), HOMO(B)->L+3(B) (5%),

					HOMO(B)->L+6(B) (5%)
24	2.5894	478.82	0.0158	H-17(B)->LUMO(B) (65%), H-11(B)->LUMO(B) (17%)	H-18(B)->LUMO(B) (2%), H-16(B)->LUMO(B) (3%), H-15(B)->LUMO(B) (7%), H-8(B)->L+1(B) (2%)
33	2.8225	439.27	0.0158	H-16(B)->L+1(B) (70%)	H-1(A)->LUMO(A) (3%), H-20(B)->L+1(B) (2%), H-17(B)->L+1(B) (4%), H-14(B)->L+1(B) (6%), H-13(B)->L+1(B) (4%), H-11(B)->L+1(B) (4%)
43	3.0349	408.52	0.0136	HOMO(B)->L+2(B) (49%), HOMO(B)->L+5(B) (28%)	HOMO(A)->L+3(A) (4%), HOMO(B)->L+3(B) (3%)
59	3.3684	368.08	0.0133		H-3(A)->L+7(A) (3%), H-3(A)->L+9(A) (6%), H-3(A)->L+10(A) (4%), H-1(A)->L+3(A) (2%), H-1(A)->L+7(A) (3%), H-1(A)->L+9(A) (5%), H-1(A)->L+10(A) (7%), H-22(B)->L+1(B) (6%), H-1(B)->L+4(B) (3%), H-1(B)->L+9(B) (3%), H-1(B)->L+10(B) (3%), H-1(B)->L+11(B) (5%), H-1(B)->L+12(B) (4%)
25	2.5985	477.14	0.0112	H-20(B)->L+1(B) (17%), H-14(B)->L+1(B) (67%)	H-19(B)->L+1(B) (4%), H-8(B)->L+1(B) (2%)
50	3.1959	387.95	0.011	H-1(A)->L+2(A) (49%)	HOMO(A)->L+2(A) (10%), H-3(A)->L+5(A) (2%), H-1(A)->L+3(A) (2%), H-22(B)->L+1(B) (3%), H-20(B)->L+1(B) (6%), H-19(B)->L+1(B) (9%), H-17(B)->L+1(B) (2%), H-1(B)->L+4(B) (2%)
47	2.2276	393.63	0.0105	HOMO(A)->L+1(A) (11%), H-21(B)->LUMO(B) (41%), HOMO(B)->L+3(B) (11%)	H-2(A)->L+1(A) (5%), H-2(A)->L+4(A) (2%), H-1(A)->L+1(A) (2%), HOMO(A)->L+3(A) (6%), H-20(B)->LUMO(B) (2%), HOMO(B)->L+6(B) (4%)

**S10:** Calculations for concentration of oxidized species in 20.5 mol% SFX-(TFSI)<sub>2</sub>, calculation carried out as per Nguyen et al<sup>2</sup> and reduction and oxidation potentials were used from the data obtained in Maciejczyk et al manuscript.<sup>3</sup>

For SFX-MeOTAD at room temperature (25 °C)



$$E_{Cell} = -5.15 - (-5.31)$$

$$E_{Cell} = 0.15 \text{ eV}$$

Calculate equilibrium constant:

$$K = e^{\frac{nFE_{Cell}}{RT}}$$

$$K = e^{\frac{1 \times 96485 \times 0.15}{8.314 \times 298}}$$

$$K = 344.2972257$$

Optimal dopant concentration of 20.5 mole% SFX-(TFSI)<sub>2</sub> used masses of 0.074g SFX-MeOTAD and 0.027g SFX-(TFSI)<sub>2</sub>. Final concentrations of the neutral SFX-MeOTAD, SFX-MeOTAD<sup>+</sup> and SFX-MeOTAD<sup>2+</sup> can then be calculated to ascertain their final concentrations in this given mixture by solving for x from the equilibrium constant.

$$K = \frac{[Products]}{[Reactants]}$$

$$K = \frac{[SFX^+]_f^2}{[SFX]_f \times [SFX^{2+}]_f}$$

$$[SFX]_f = [SFX]_i - x$$

$$[SFX]_f = \frac{0.07402}{1241.43} - x$$

$$[SFX]_f = 5.962478754 \times 10^{-5} - x$$

$$[SFX^+]_f = 2x$$

$$[SFX^{2+}]_f = [SFX^{2+}]_i - x$$

$$[SFX^{2+}]_f = \frac{0.027701}{1801.73} - x$$

$$[SFX^{2+}]_f = 1.537466768 \times 10^{-5} - x$$

$$\frac{[SFX^+]_f^2}{[SFX]_f \times [SFX^{2+}]_f} = 344.2972257$$

$$\frac{[2x][2x]}{[5.962478754 \times 10^{-5} - x][1.537466768 \times 10^{-5} - x]} = 344.2972257$$

$$\frac{4x^2}{9.167112939 \times 10^{-10} - 5.962478754 \times 10^{-5}x - 1.537466768 \times 10^{-5}x + x^2} = 344.2972257$$

$$\frac{4x^2}{9.167112939 \times 10^{-10} - 7.499945522 \times 10^{-5}x + x^2} = 344.2972257$$

$$4x^2 = 344.2972257[9.167112939 \times 10^{-10} - 7.499945522 \times 10^{-5}x + x^2]$$

$$4x^2 = 3.156211553 \times 10^{-7} - 0.02582210436x + 344.2972257x^2$$

$$340.2972257x^2 - 0.02582210436x + 3.156211553 \times 10^{-7} = 0$$

Using the quadratic formula and solving for x found that when x is calculated to be  $1.531318679 \times 10^{-5}$  this gave positive values for the final concentrations of SFX-MeOTAD, SFX-MeOTAD<sup>+</sup> and SFX-MeOTAD<sup>2+</sup>.

$$[SFX]_f = 5.962478754 \times 10^{-5} - x$$

$$[SFX]_f = 5.962478754 \times 10^{-5} - 1.531318679 \times 10^{-5} = 4.431160075 \times 10^{-5}$$

$$[SFX^+]_f = 2x$$

$$[SFX^+]_f = 2 \times 1.531318679 \times 10^{-5} = 3.062637358 \times 10^{-5}$$

$$[SFX^{2+}]_f = 1.537466768 \times 10^{-5} - x$$

$$[SFX^{2+}]_f = 1.537466768 \times 10^{-5} - 1.531318679 \times 10^{-5} = 6.148089 \times 10^{-8}$$

$$SFX \text{ mol \%} = \frac{[SFX]_f}{[SFX]_f + [SFX^+]_f + [SFX^{2+}]_f} \times 100$$

$$SFX \text{ mol \%} = \frac{4.431160075 \times 10^{-5}}{4.431160075 \times 10^{-5} + 3.062637358 \times 10^{-5} + 6.148089 \times 10^{-8}} \times 100$$

$SFX \text{ mol \%} = 59.08\%$

$$SFX^+ \text{ mol \%} = \frac{[SFX^+]_f}{[SFX]_f + [SFX^+]_f + [SFX^{2+}]_f} \times 100$$

$$SFX^+ \text{ mol \%} = \frac{3.062637358 \times 10^{-5}}{4.431160075 \times 10^{-5} + 3.062637358 \times 10^{-5} + 6.148089 \times 10^{-8}} \times 100$$

$SFX^+ \text{ mol \%} = 40.84\%$

$$SFX^{2+} \text{ mol \%} = \frac{[SFX^{2+}]_f}{[SFX]_f + [SFX^+]_f + [SFX^{2+}]_f} \times 100$$

$$SFX^{2+} \text{ mol \%} = \frac{6.148089 \times 10^{-8}}{4.431160075 \times 10^{-5} + 3.062637358 \times 10^{-5} + 6.148089 \times 10^{-8}} \times 100$$

$SFX^{2+} \text{ mol \%} = 0.08\%$

**S11:** Fitting parameters extracted from C1s core level XPS spectra of undoped SFX-MeOTAD [0%], SFX-MeOTAD doped with different concentration of SFX(TFSI)<sub>2</sub> [10% and 20%] and, pure SFX(TFSI)<sub>2</sub> [100%] samples.

Sample	Region	Component	Peak position ± 0.2 eV	FWHM ± 0.1 eV	Atomic % ± 0.1
0%	C1s	C-H	284.5	1.8	46.7
		C=C/C-C	285.4	1.7	29.3
		C-N/C-O	286.4	1.6	18.8
		C <sub>a</sub> -O-C	287.5	1.5	3.7
		π-π*	291.6	2.4	1.4
	N1s	Amine N	399.5	2.0	100.0
	O1s	C <sub>a</sub> -O	532.3	2.5	100.0
10%	C1s	C-H	284.5	1.6	41.4
		C=C/C-C	285.3	1.5	28.2
		C-N/C-O	286.2	1.6	19.4
		C <sub>a</sub> -O-C	287.0	1.7	8.4
		π-π* + CF <sub>3</sub>	291.8	2.5	2.6
	N1s	Amine N	399.5	1.8	100.0
	O1s	C <sub>a</sub> -O	532.4	2.2	100.0
20%	C1s	CF <sub>3</sub>	688.0	2.4	100.0
		C-H	284.6	1.6	45.4
		C=C/C-C	285.5	1.6	33.7
		C-N/C-O	286.5	1.5	14.8
		C <sub>a</sub> -O-C	287.5	1.5	2.9
	π-π* + CF <sub>3</sub>		291.7	2.7	3.1

	N1s	Amine N	399.5	1.8	100.0
	O1s	C <sub>a</sub> -O	532.4	2.3	100.0
	F1s	CF <sub>3</sub>	688.0	2.3	100.0
100%	C1s	C-H	284.6	1.9	41.6
		C=C/C-C	285.6	1.6	29.5
		C-N/C-O	286.6	1.5	15.8
		C <sub>a</sub> -O-C	287.6	1.7	6.8
		$\pi-\pi^* + CF_3$	292.8	2.5	6.3
	N1s	Amine N	399.5	2.0	79.0
		NO <sub>x</sub>	402.2	2.1	21.0
	O1s	C <sub>a</sub> -O	532.4	2.5	100.0
	F1s	CF <sub>3</sub>	688.0	2.3	100.0

Where C<sub>a</sub> corresponds to the aromatic carbon.

**S12:** Peak positions and assignments of the C *K*-edge resonances of pristine and doped SFX-MeOTAD.

Peak position $\pm 0.2$ eV	Assignment	Reference
285.6	$1s \rightarrow \pi_1^*(C_{2,3}) + 1s \rightarrow \pi_2^*(C_{2,3,4})$	4-7
286.7	$1s \rightarrow \pi_2^*(C_1) + 1s \rightarrow \pi^*$ transition of aryl-O + $\pi^* C-N$	4,5,8-13
287.5	$C1s \rightarrow \pi^*(C-H) + C1s \rightarrow \sigma^* C-H/3p$ Rydberg-like excitations	4,5,13-17
289.0	$C1s \rightarrow \pi_3^*(C_{2,3,4}) + \sigma^*(C-H)$	4-6
290.6	$C1s \rightarrow \pi_3^*(C_1)$	4-6
292.2	$C1s \rightarrow \sigma^*(C-C + C-O + C-N)$	9,14,16-18
294.2	$C1s \rightarrow \sigma_1^*(C-C) + C1s \rightarrow \sigma^*(e_{2g} + a_{2g}) + \pi^*$ shake-up feature	4-7,19
298.6	$C1s \rightarrow \sigma^*(C-O)$	20
303.2	$C1s \rightarrow \sigma_2^*(C=C)$	4-6,17

Where  $C_{2,3}$  and  $C_1$  signify the position of the carbon atoms on the benzene ring.

**S13:** Peak positions and assignments of the N *K*-edge NEXAFS resonances of hole conductor molecules (pristine and doped).

Peak position $\pm 0.2$ eV	Assignment	Reference
402.5	N1s $\rightarrow\pi^*$ (Pyrrole N) + $\pi^*$ (amine N)	18,21
403.2	N1s $\rightarrow\pi^*$ (Pyrrole N)	18
407.3	N1s $\rightarrow\sigma^*$ (N-C)	16,18,22
411.5	N1s $\rightarrow\sigma^*$ (N=C, N-C)	12,16,17

## References

- 1 N. M. O'Boyle, A. L. Tenderholt and K. M. Langner, *J. Comput. Chem.*, 2008, **29**, 839–845.
- 2 W. H. Nguyen, C. D. Bailie, E. L. Unger and M. D. Mcgehee, *J. Am. Chem. Soc.*, 2014, **136**, 10996–11001.
- 3 M. Maciejczyk, A. Ivaturi and N. Robertson, *J. Mater. Chem. A*, 2016, **4**, 4855–4863.
- 4 J. L. Solomon, R. J. Madix and J. Stohr, *Surf. Sci.*, 1991, 255, 12–30.
- 5 J. A. Horsley, J. Stöhr, A. P. Hitchcock, D. C. Newbury, A. L. Johnson and F. Sette, *J. Chem. Phys.*, 1985, 83, 6099.
- 6 S. X. Huang, D. A. Fischer and J. L. Gland, *J. Phys. Chem.*, 1996, **100**, 10223–10234.
- 7 S. Aminipoor, L. Becker, B. Hillert and J. Haase, *Surf. Sci.*, DOI:10.1016/0039-6028(91)90489-F.
- 8 C. K. Boyce, G. D. Cody, M. Feser, C. Jacobsen, A. H. Knoll and S. Wirick, *Geology*, 2002, **30**, 1039–1042.
- 9 O. Dhez, H. Ade and S. G. Urquhart, *J. Electron Spectros. Relat. Phenomena*, 2003, **128**, 85–96.
- 10 Y. Zubavichus, A. Shaporenko, M. Grunze and M. Zharnikov, *J. Phys. Chem. A*, 2005, **109**, 6998–7000.
- 11 E. Apen, A. P. Hitchcock and J. L. Gland, *J. Phys. Chem.*, 1993, **97**, 6859–6866.
- 12 R. V. Dennis, B. J. Schultz, C. Jaye, X. Wang, D. a. Fischer, A. N. Cartwright and S. Banerjee, *J. Vac. Sci. Technol. B*, 2013, **31**, 041204.
- 13 Dawit Solomon, Johannes Lehmann, James Kinyangi, Binqing Liang, Karen Heymann, Lena Dathe, Kelly Hanley, Sue Wirick and Chris Jacobsen, *Soil Sci. Soc. Am. J.*, 2008, **73**, 1817–1830.
- 14 S. Sainio, D. Nordlund, R. Gandhiraman, H. Jiang, || J Koehne, J. Koskinen, ⊥ M Meyyappan and T. Laurila, *J. Phys. Chem. C*, 2016, **120**, 22655–22662.
- 15 D. Solomon, J. Lehmann, J. Kinyangi, B. Liang and T. Schä, *J. Am. soil Sci. Soc.*, 2005, **69**, 107–119.
- 16 N. Graf, E. Yegen, T. Gross, A. Lippitz, W. Weigel, S. Krakert, A. Terfort and W. E. S.

- Unger, *Surf. Sci.*, 2009, **603**, 2849–2860.
- 17 A. G. Shard, J. D. Whittle, A. J. Beck, P. N. Brookes, N. A. Bullett, R. A. Talib, A. Mistry, D. Barton and S. L. McArthur, *J. Phys. Chem. B*, 2004, **108**, 12472–12480.
- 18 K. G. Latham, M. I. Simone, W. M. Dose, J. A. Allen and S. W. Donne, *Carbon N. Y.*, 2017, **114**, 566–578.
- 19 K. H. H. W.H.E. Schwarz, T.C. Chang, U. Seeger, *Chem. Phys.*, 1987, **117**, 73–89.
- 20 S. Banerjee, T. Hemraj-benny, M. Balasubramanian, D. A. Fischer, J. A. Misewich, S. S. Wong, S. S. Brook, S. Brook, W. Lafayette and A. December, *Chem Commun*, 2004, 772–773.
- 21 B. J. Schultz, R. V Dennis, J. P. Aldinger, C. Jaye, X. Wang, D. a Fischer, A. N. Cartwright and S. Banerjee, *RSC Adv.*, 2014, **4**, 634–644.
- 22 A. Marchioro, J. Teuscher, D. Friedrich, M. Kunst, R. Van De Krol, T. Moehl, M. Grätzel and J. E. Moser, *Nat. Photonics*, 2014, **8**, 250–255.